2021

# Effect of CO2 flooding on the wettability evolution of sand-stone

Cut Aja Fauziah

Ahmed Al-Yaseri

Emad Al-Khdheeawi

Nilesh Kumar Jha

Hussein R. Abid
*Edith Cowan University*

*See next page for additional authors*



10.3390/en14175542
Fauziah, C. A., Al-Yaseri, A., Al-Khdheeawi, E., Jha, N. K., Abid, H. R., Iglauer, S., . . . Barifcani, A. (2021). Effect of CO2 flooding on the wettability evolution of sand-stone. *Energies, 14*(17), Article 5542.
https://doi.org/10.3390/en14175542

energies

MDPI

*Article*

# Effect of $CO_2$ Flooding on the Wettability Evolution of Sand-Stone

**Cut Aja Fauziah [1], Ahmed Al-Yaseri [1,2,*], Emad Al-Khdheeawi [3], Nilesh Kumar Jha [4], Hussein Rasool Abid [1,5,6,*], Stefan Iglauer [5], Christopher Lagat [1] and Ahmed Barifcani [1]**

1 Western Australia School of Mines: Minerals, Energy and Chemical Engineering, Discipline of Petroleum Engineering, Curtin University, Kensington 6151, Australia; cutaja.fauziah@postgrad.curtin.edu.au (C.A.F.); christopher.lagat@curtin.edu.au (C.L.); A.Barifcani@curtin.edu.au (A.B.)
2 Petroleum Engineering Department, School of Engineering, Australian College of Kuwait, Kuwait 13015, Kuwait
3 Petroleum Technology Department, University of Technology, Baghdad 10071, Iraq; e.al-khdheeawi@postgrad.curtin.edu.au
4 School of Petroleum Technology, Pandit Deendayal Petroleum University, Raisan, Gandhinagar 382007, India; nilesh.jha@spt.pdpu.ac.in
5 School of Engineering, Edith Cowan University, Joondalup 6027, Australia; s.iglauer@ecu.edu.au
6 Environmental Department, Applied Medical Science, University of Karbala, Karbala 56001, Iraq
* Correspondence: ahmed.al-yaseri@curtin.edu.au (A.A.-Y.); hussein.abid@curtin.edu.au (H.R.A.)

**Abstract:** Wettability is one of the main parameters controlling $CO_2$ injectivity and the movement of $CO_2$ plume during geological $CO_2$ sequestration. Despite significant research efforts, there is still a high uncertainty associated with the wettability of $CO_2$/brine/rock systems and how they evolve with $CO_2$ exposure. This study, therefore, aims to measure the contact angle of sandstone samples with varying clay content before and after laboratory core flooding at different reservoir pressures, of 10 MPa and 15 MPa, and a temperature of 323 K. The samples' microstructural changes are also assessed to investigate any potential alteration in the samples' structure due to carbonated water exposure. The results show that the advancing and receding contact angles increased with the increasing pressure for both the Berea and Bandera Gray samples. Moreover, the results indicate that Bandera Gray sandstone has a higher contact angle. The sandstones also turn slightly more hydrophobic after core flooding, indicating that the sandstones become more $CO_2$-wet after $CO_2$ injection. These results suggest that $CO_2$ flooding leads to an increase in the $CO_2$-wettability of sandstone, and thus an increase in vertical $CO_2$ plume migration and solubility trapping, and a reduction in the residual trapping capacity, especially when extrapolated to more prolonged field-scale injection and exposure times.

**Keywords:** $CO_2$ injectivity; wettability; contact angle; sandstone; $CO_2$ sequestration



**Citation:** Fauziah, C.A.; Al-Yaseri, A.; Al-Khdheeawi, E.; Jha, N.K.; Abid, H.R.; Iglauer, S.; Lagat, C.; Barifcani, A. Effect of $CO_2$ Flooding on the Wettability Evolution of Sand-Stone. *Energies* **2021**, *14*, 5542. https://doi.org/10.3390/en14175542

Academic Editor: João Fernando Pereira Gomes

Received: 23 July 2021
Accepted: 31 August 2021
Published: 5 September 2021



## 1. Introduction

Carbon geological sequestration (CGS) has been proposed as an efficient method to reduce anthropogenic $CO_2$ emissions into the atmosphere and thus mitigate global climate change [1]. In essence, the technique involves capturing $CO_2$ from large stationary emission sources and locking it into some natural geological formations [1–3]. There are three geological formations that have attained a wide consideration. They include (1) depleted oil and gas reservoir, (2) deep saline aquifers, and (3) coal seams [1]. In saline aquifers and oil and gas reservoirs, $CO_2$ storage is typically placed at depths below 800 m, where $CO_2$ becomes liquid or supercritical because of the ambient pressure and temperature conditions [1]. Therefore, the vertical migration of $CO_2$ is the main problem involved in $CO_2$ injection due to the density differences between the brine and $CO_2$ [4,5]. It is also essential to assess the different functional trapping mechanisms, which prevent the buoyant $CO_2$ from flowing upwards [1]. The $CO_2$ can be trapped in geological formations utilising

four mechanisms, including structural trapping [6,7], capillary trapping [8–11], solubility trapping [12–14], and mineral trapping [15–17]. Furthermore, coal seams are considered as another option for the underground storage, in which the $CO_2$ injection into coal seams will have advantages for both $CO_2$ storage and enhance methane recovery [1,2]. A number of large-scale $CO_2$ storage projects are currently in operation worldwide. These have captured and stored millions of tonnes of $CO_2$ annually. Many more projects have been planned. Specifically, oil and gas companies have been operating geological $CO_2$ storage projects for a number of years. They have successfully demonstrated that securely storing a large quantity of $CO_2$ in a deep underground area is possible [1]. For instance, the active CGS projects are (1) Sleipner (Norway), (2) Weyburn Midale (Canada), and (3) Cranfield (US), established in 1996, 2000, and 2008, with $CO_2$ capture capacities of 1, 3, and 1.5 Mt/year, respectively. The planned CGS projects include (1) Gorgon (Australia), (2) Quest (Canada), and (3) GreenGen (China), established in 2016, 2015, and 2011, respectively [1,5].

In carbon geo-sequestration, wettability is a crucial factor that intensely and directly influences containment security, injectivity, structural, dissolution, and residual trapping capacities [18,19]. Five different wettability states can be conceptualised in a real reservoir, i.e., strongly water-wet, weakly water-wet, intermediate-wet, weakly $CO_2$-wet, and strongly $CO_2$-wet (where complete wetting occurs), with approximate contact angles of 0°–50°, 50°–70°, 70°–110°, 110°–130°, and 130°–180°, respectively [20]. These differences in wettability are caused by geological and chemical factors, such as surface chemistry (e.g., organic content) [21–23], reservoir pressure (the increase in pressure leads to a decrease in water wettability) [18,24,25], reservoir temperature [26–28], salinity, and ion type (salinity increases as $CO_2$ wettability increases) [18,29–32]. Therefore, it is essential to understand the fluid-rock interaction, as these interactions clearly can affect the capillary pressure and aquifer permeability, and hence the injectivity and storage capacities [33,34].

Injected $CO_2$ forms carbonic acid in the brine phase [35,36]. It interacts with rock minerals, which leads to mineral alterations and ion dissolution–precipitation [37]. Deep saline sandstone reservoirs are potential candidates for $CO_2$ sequestration [1]. Sandstones generally consist of siliceous minerals, clays, and various carbonates, along with quartz [38]. These minerals react differently to the changing environment when $CO_2$ is injected, e.g., calcite cement is highly reactive in an acidic environment [35,39,40]. In fact, pH decreases to 3–4 when $CO_2$ mixes with brine at reservoir conditions [41,42], and such an acidic condition can considerably affect the permeability and pore morphology [43]. Alternatively, $CO_2$ can be stuck in the target reservoir's pore space for hundreds or thousands of years because of the slow dissolution kinetics caused by the partial mixing of $CO_2$ and brine [44].

Some studies have reported that such water–$CO_2$–rock interactions could change the sandstone pore structures due to fines migration and precipitation or reaction with sensitive materials [45,46]. Such a change can strongly affect the rock porosity and permeability performance [36,47,48]. Furthermore, the influence of the temperature and injection rate on the permeability reduction after $CO_2$ injection have been examined on Berea sandstone [36] and sandstones from the Pembina Cardium field, Canada [49], whereas other studies investigated the factors controlling the permeability changes in sandstone during core flooding [50]. However, the effect of $CO_2$ injection on the wettability changes has received less attention. Thus, this study analyses how $CO_2$ injection changes sandstone's wettability. This change was correlated with a microstructural alteration in the sandstone caused by $CO_2$ flooding. Subsequently, we determined how $CO_2$ flooding affects the $CO_2$ trapping capacities (i.e., residual and dissolution) and the amount of free $CO_2$ in saline aquifers (i.e., mobile $CO_2$).

## 2. Materials and Methods

### *2.1. Materials*

Two homogeneous Berea sandstone samples (low clay content) and two Bandera Gray (high clay content) were used in this study. The sandstones were thoroughly characterised by scanning electron microscopy (SEM) to measure the surface morphology and

quantitative X-ray diffraction (XRD—Bruker-AXS D8) to measure the mineral composition before/after the flooding experiment. The samples' petrophysical properties, including porosity and permeability, were measured before and after flooding and are reported in Table 1.

**Table 1.** Petrophysical and mineralogical sandstone properties.

| Sample | Porosity [a] (%) | Brine Permeability (mD) | Length (mm) | Diameter (mm) | Mineral Constituents [b] | |
|---|---|---|---|---|---|---|
| | | | | | Mineral | wt% |
| **Before Flooding** | | | | | | |
| Berea | 20 | 69 | 50.88 | 30.78 | Quartz | 84.3 |
| | | | | | Kaolinite | 4.1 |
| | | | | | Illite | 1.9 |
| | | | | | Albite | 4.2 |
| | | | | | Microcline | 4.1 |
| | | | | | Chlorite | 1.4 |
| Bandera Gray | 19 | 9 | 60.32 | 30.80 | Quartz | 58.2 |
| | | | | | Kaolinite | 3.2 |
| | | | | | Illite | 3.6 |
| | | | | | Albite | 12.4 |
| | | | | | Muscovite | 1.6 |
| | | | | | Chlorite | 5.7 |
| | | | | | Ankerite | 15.3 |
| **After Flooding** | | | | | | |
| Berea | 22 | 80 | 50.88 | 30.78 | Quartz | 84.9 |
| | | | | | Kaolinite | 3.9 |
| | | | | | Illite | 1.8 |
| | | | | | Albite | 4.2 |
| | | | | | Microcline | 4.1 |
| | | | | | Chlorite | 1.1 |
| Bandera Gray | 20 | 7.3 | 60.32 | 30.80 | Quartz | 58.4 |
| | | | | | Kaolinite | 3.1 |
| | | | | | Illite | 3.2 |
| | | | | | Albite | 12.2 |
| | | | | | Muscovite | 3.1 |
| | | | | | Chlorite | 5.2 |
| | | | | | Ankerite | 14.8 |

[a] Porosity was measured with AP-608 Coretest Instrument. [b] The mineral composition of the samples was measured by X-ray Diffraction (XRD)Bruker—AXS D8.

### 2.2. $CO_2$ Core Flooding Experiment

The Berea and Bandera Gray core plugs were wrapped in polytetrafluoroethylene (PTFE) tape, aluminium foil, and PTFE tape again to be prepared for plugging. Subsequently, the samples were sealed with a PTFE heat-shrink sleeve and were placed in a rubber sleeve in a high-pressure and a high-temperature core holder (Figure 1). The samples were next vacuumed for more than 20 h [50]. In the next step, the sandstone samples were saturated with dead brine (5 wt% NaCl and 1 wt% KCL) using a high-precision syringe pump (ISCO 500D). The dead brine was then displaced by 5 pore volumes of live brine (5 wt% NaCl and 1 wt% KCL equilibrated with $CO_2$) at 1 mL/min [51]. The injection rate was reduced to 0.05 mL/min, and the injection continued for 7 days at reservoir conditions (pore pressure of 10 MPa, confining pressure of 15 MPa, and temperature of 323 K). This simulates the sinking of $CO_2$-saturated brine deep into the reservoir, i.e., the dissolution trapping [52–54]. Finally, five-pore volumes of supercritical $CO_2$ ($scCO_2$) were injected to displace the live brine and to simulate the $CO_2$ injection into the reservoir. Figure 1 presents a schematic of the core flooding apparatus used in this study.

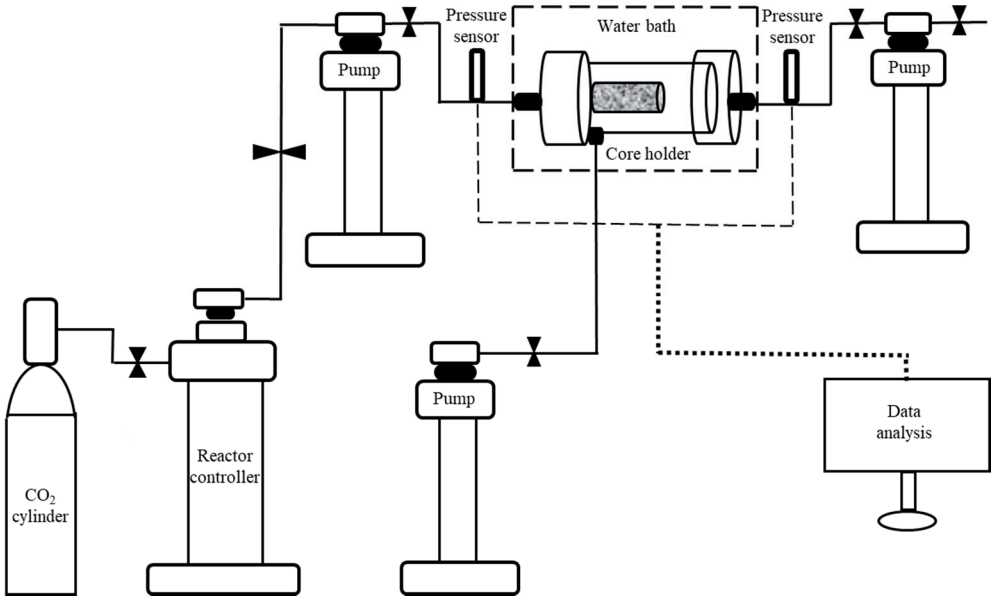


**Figure 1.** Schematic of the core flooding system (modified from [50]).

### *2.3. Contact Angle Measurements*

For the $CO_2$–wettability tests, the samples were cut with a high-speed diamond blade (5 mm thick cuboids, with a 38 mm diameter), and each sample was exposed to air plasma (model Diener plasma, Ebhausen, Germany, Yocto) for 5 min to remove any potential organic surface contaminations [55,56]. Subsequently, the contact angle was measured using the tilted plate method (as it can quantify simultaneously the advancing and receding contact angles) [57] at storage conditions. For contact angle measurements, the sample was placed inside the pressure cell at a set temperature (323 °K). $CO_2$ pressure was raised to the desired pressure (10 MPa and 15 MPa), using a high precision syringe pump (model ISCO 500D; pressure accuracy of 0.1% FS). A droplet of the brine (5 wt% NaCl and 1 wt% KCl in deionised water) with an average volume of ~6 µL ± 1 µL was released onto the tilted (tilted angle of 12°) sample (Berea and Bandera Gray) surface through a needle. The advancing and receding contact angles were then calculated at the leading and trailing edge. A high-resolution video camera (with specification of Basler scA (640–70) fm, pixel size = 7.4 µm; frame rate = 71 frames per second; Fujinon CCTV lens: HF35HA-1B; 1.6/35 mm) recorded the whole process and the images extracted from the video files to measure the contact angles. Figure 2 illustrates the experimental setup of contact angle measurement. The standard deviation in the contact angle result was determined as ±3° based on replicated measurements.

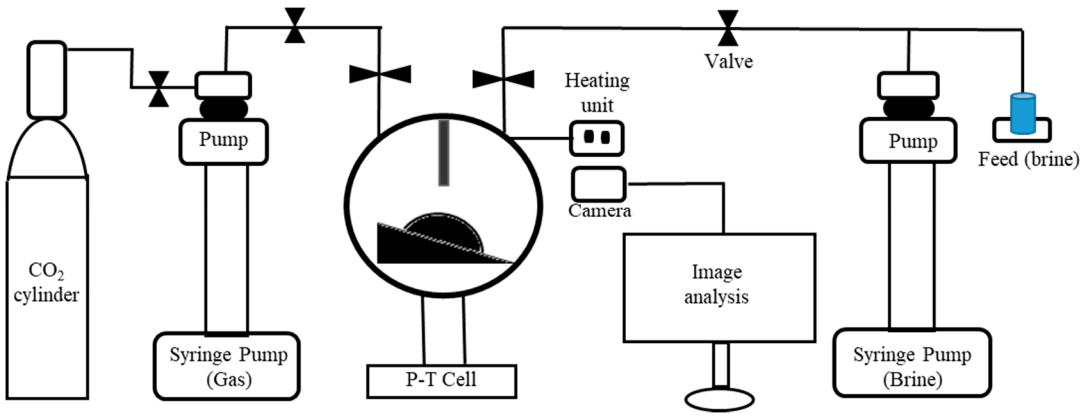


**Figure 2.** The experimental setup for the contact angle measurement (modified from [58]).

## 3. Results and Discussion

### *3.1. Controlling Factors on Sandstone Wettability*

The wettability of sandstone samples (Berea with low clay content and Bandera Gray with high clay content) was measured before and after $CO_2$ flooding at 10 and 15 MPa at a constant temperature of 323 K. The results clearly indicate that the contact angles after flooding were higher than before the flooding for both samples. This shows that Berea and Bandera Gray sandstones became more $CO_2$-wet after $CO_2$ injection. Besides, the advancing and receding contact angles increased with the increasing pressure for both the Berea and Bandera Gray samples (Figure 3), which is consistent with the literature data [18,20,59,60]. As an example, the advancing contact angle of Bandera Gray before flooding increased from 86° to 105° at 323 K, for a pressure of 10 MPa and 15 MPa, respectively. The results also indicate that Bandera Gray has a higher contact angle, compared with Berea, for all test pressures and both before and after $CO_2$ flooding conditions.

Clay minerals can be distributed in different ways within the reservoirs—in the form of laminations in between the grains (laminar clays), dispersed in the reservoir, or structurally coating the grains (structural clays) [50,61,62]. Moreover, the specific clay type is also crucial in controlling the petro-physical properties of sandstone [62–64]. The scanning electron microscopy (SEM) and XRD analysis revealed that the Berea and Bandera Gray sandstones comprise different clay types and distributions. The clay types present in both sandstone samples are shown in Table 1. Studies by other researchers have also demonstrated that, besides smectite, all clay minerals adsorb significant amounts of $CO_2$ [65]. As seen from the SEM analysis, both sandstone samples contain the $CO_2$-adsorbing clays. Therefore, the high contact angle in Bandera Gray ($CO_2$-wet) is attributed to its high clay content.

Moreover, changes in albite and ankerite surfaces have been reported earlier [66]. Dissolution textures have been shown on the surfaces of detrital albite grains. Smooth surface and step-like structures of ankerite grains showed corrosion pits at grain boundaries post-experiment [66]. The dissolution of illite and chlorite can also occur [67], and chlorite dissolution following a subsequent reaction with pre-existing calcite can lead to kaolinite and $CO_2$-rich ankerite production [68]. Since the presence of calcite and its dissolution is a rate-limiting step of this reaction, kaolinite and ankerite production and their precipitation depend on the calcite content of the rock samples [68]. Kaolinite precipitation was reported earlier [66] and was evident in this work for both the Berea and Bandera Grey samples (Figures 4 and 5). Kaolinite precipitation can also be due to the interaction between $CO_2$-saturated brine and feldspar (k-feldspar, albite, microcline) present in the rock [66]. Thus, it can be inferred that a larger content of albite and ankerite in Bandera Gray samples is responsible for more significant interactions with $CO_2$-saturated brine. This phenomenon explains the higher brine contact angle, and thus the higher $CO_2$ wetting, for Bandera Gray as compared to Berea sandstone at the same conditions.

The XRD results (Figure 6) and XRD images (Figure 7) were also employed, showing no significant change in mineral composition before and after $CO_2$ flooding. This can be due to the dissolution of minerals corresponding to their stoichiometry, keeping the overall mineralogy unchanged (or with an insignificant change beyond the detection limit). The additional peak in the XRD results after the experiments corresponds to NaCl, and thus salt precipitation post-drying cannot be ruled out.

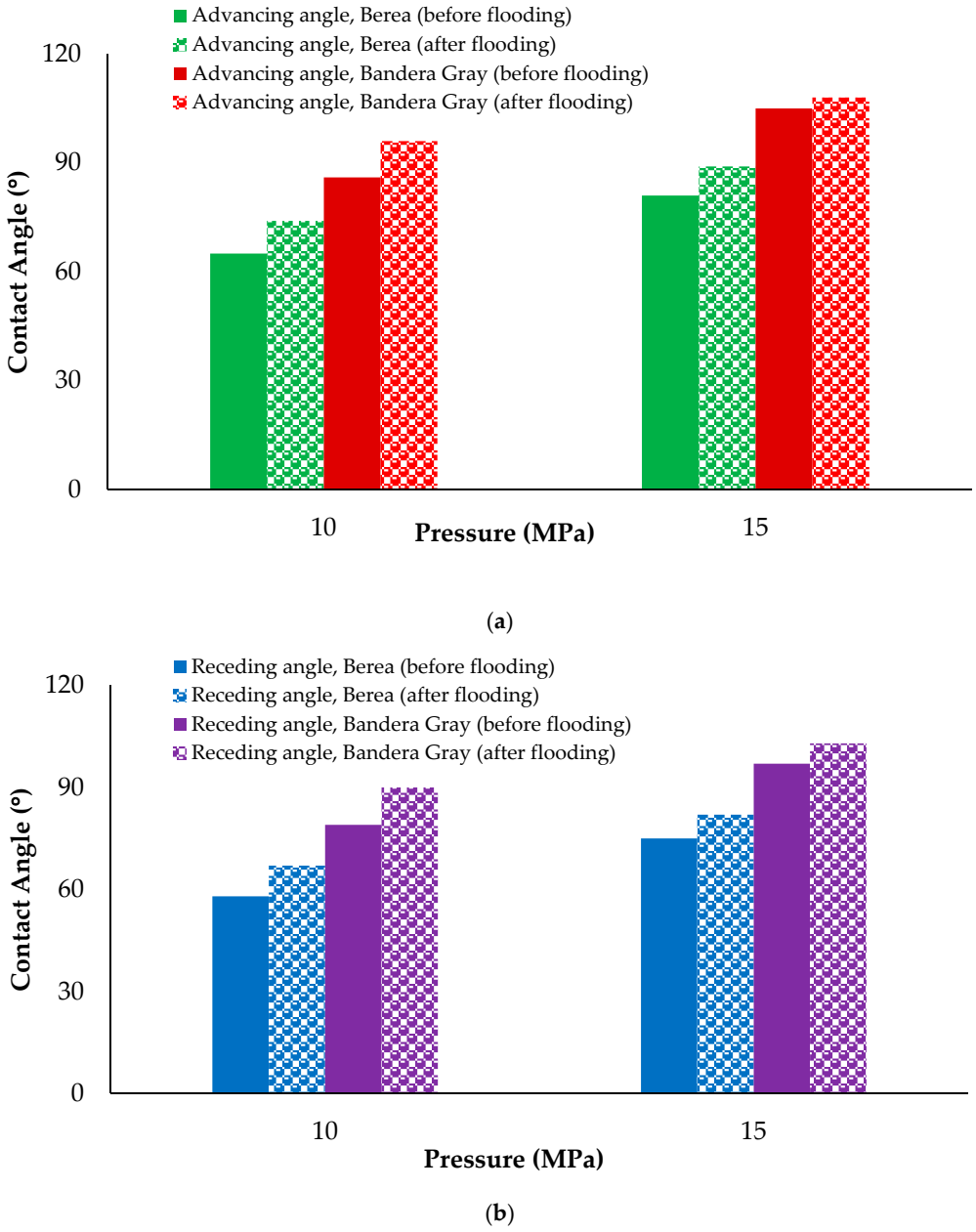


**Figure 3.** Berea and Bandera Gray sandstone/$CO_2$/brine advancing (**a**) and receding (**b**) contact angles as a function of pressure (measured at 10 and 15 MPa, and 323 K).

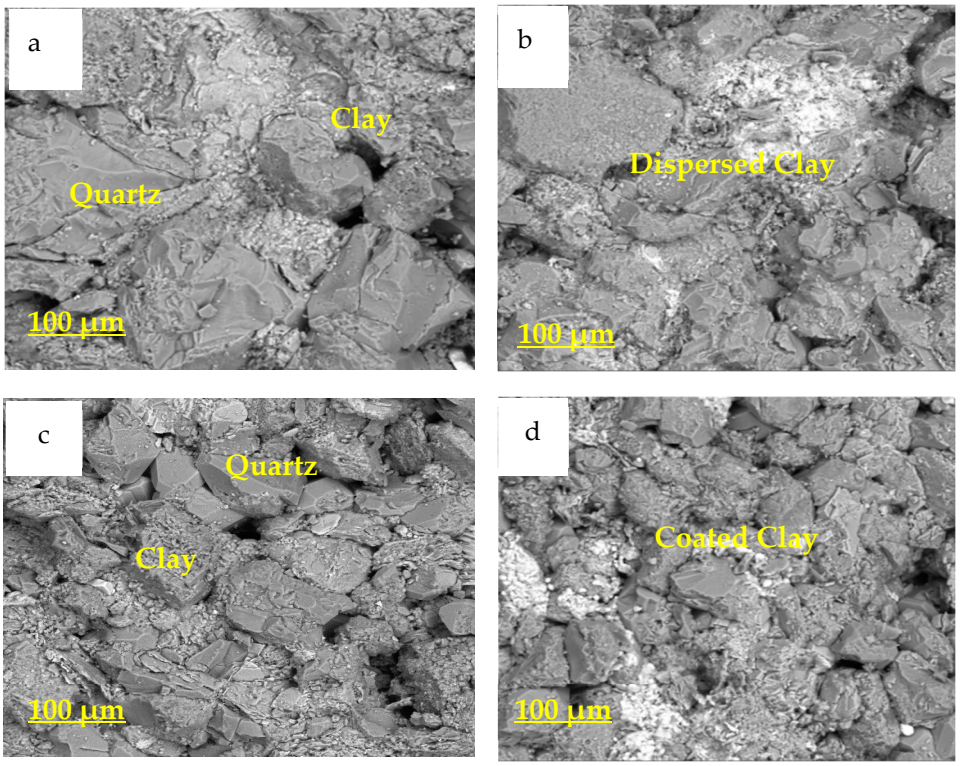


**Figure 4.** SEM images of (**a**) Berea before flooding (**b**) Berea after flooding: pore filling dispersed clay (illite/kaolinite based on the XRD) (**c**) Bandera Gray before flooding (**d**) Bandera Gray after flooding, quartz-grain-coated structural clay (mostly chlorite based on the XRD).

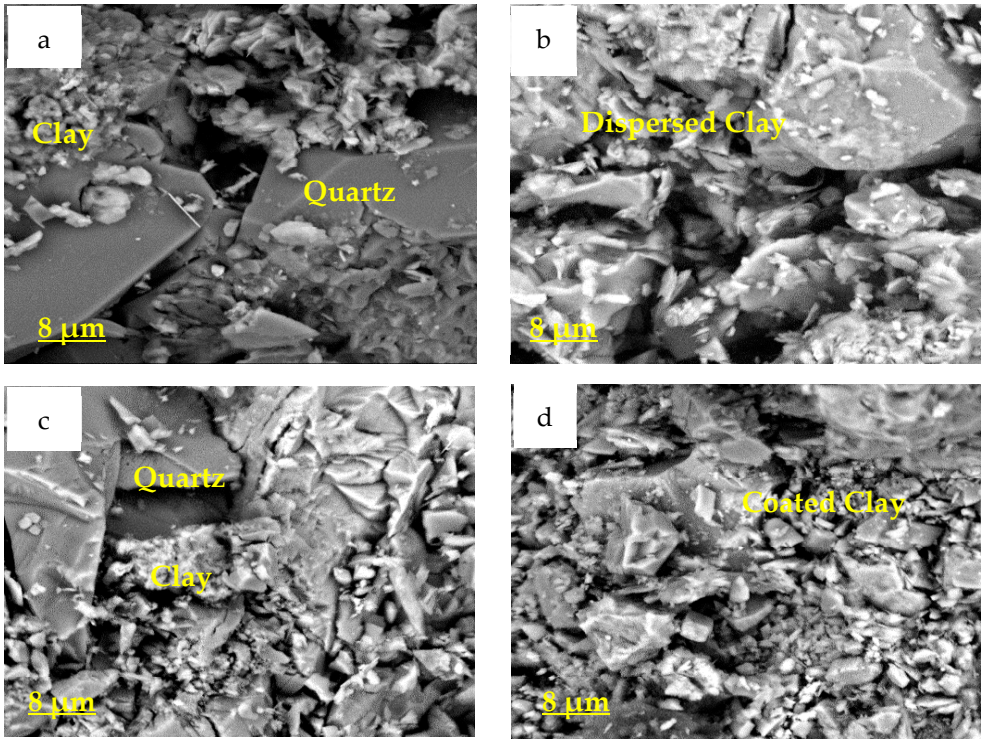


**Figure 5.** SEM images of (**a**) Berea before flooding, smooth surface (**b**) Clutter Berea after flooding: pore filling dispersed clay (**c**) Bandera Gray before flooding (**d**) Clutter Bandera Gray after flooding, quartz-grain-coated structural clay.

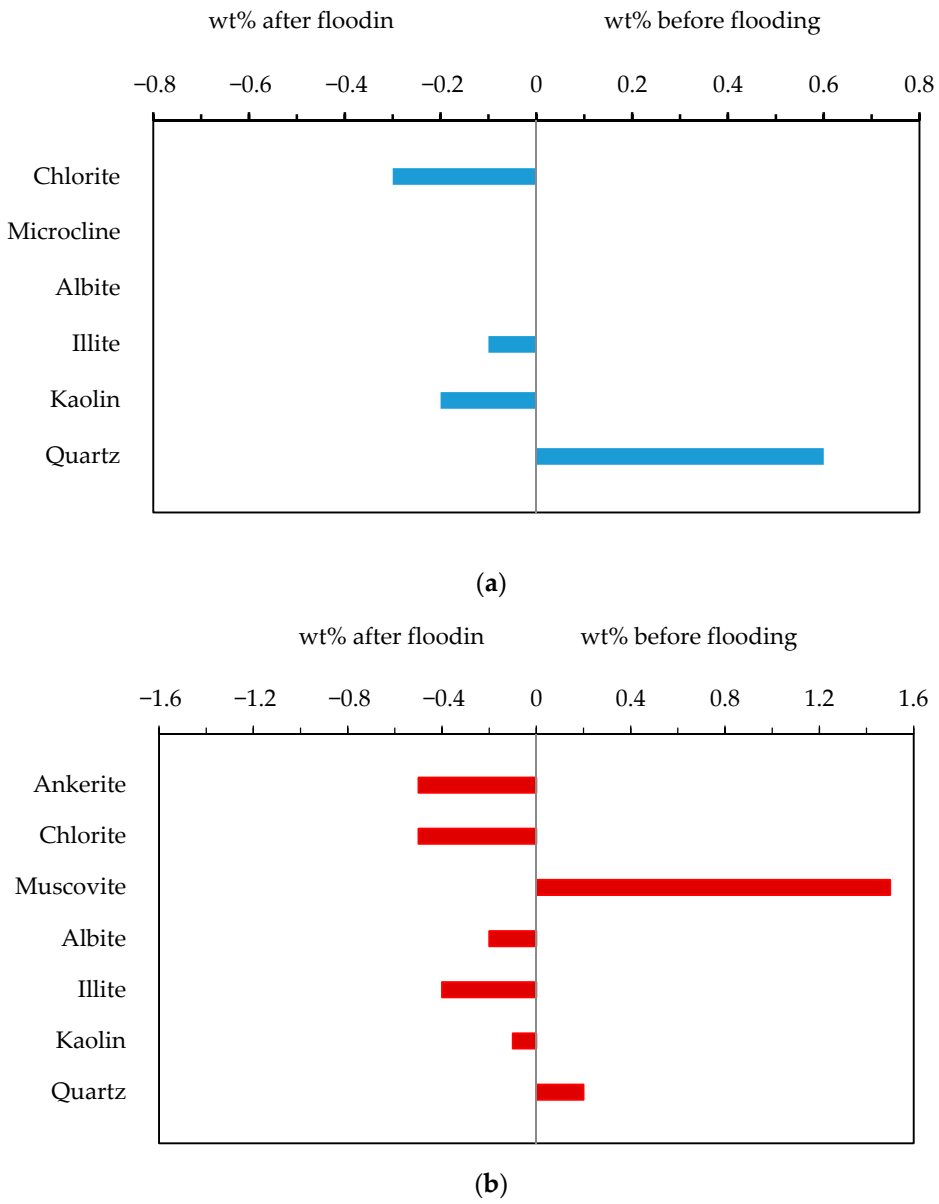


**Figure 6.** Differences in mineral compositions due to $CO_2$ flooding in: (**a**) Berea, (**b**) Bandera Gray.

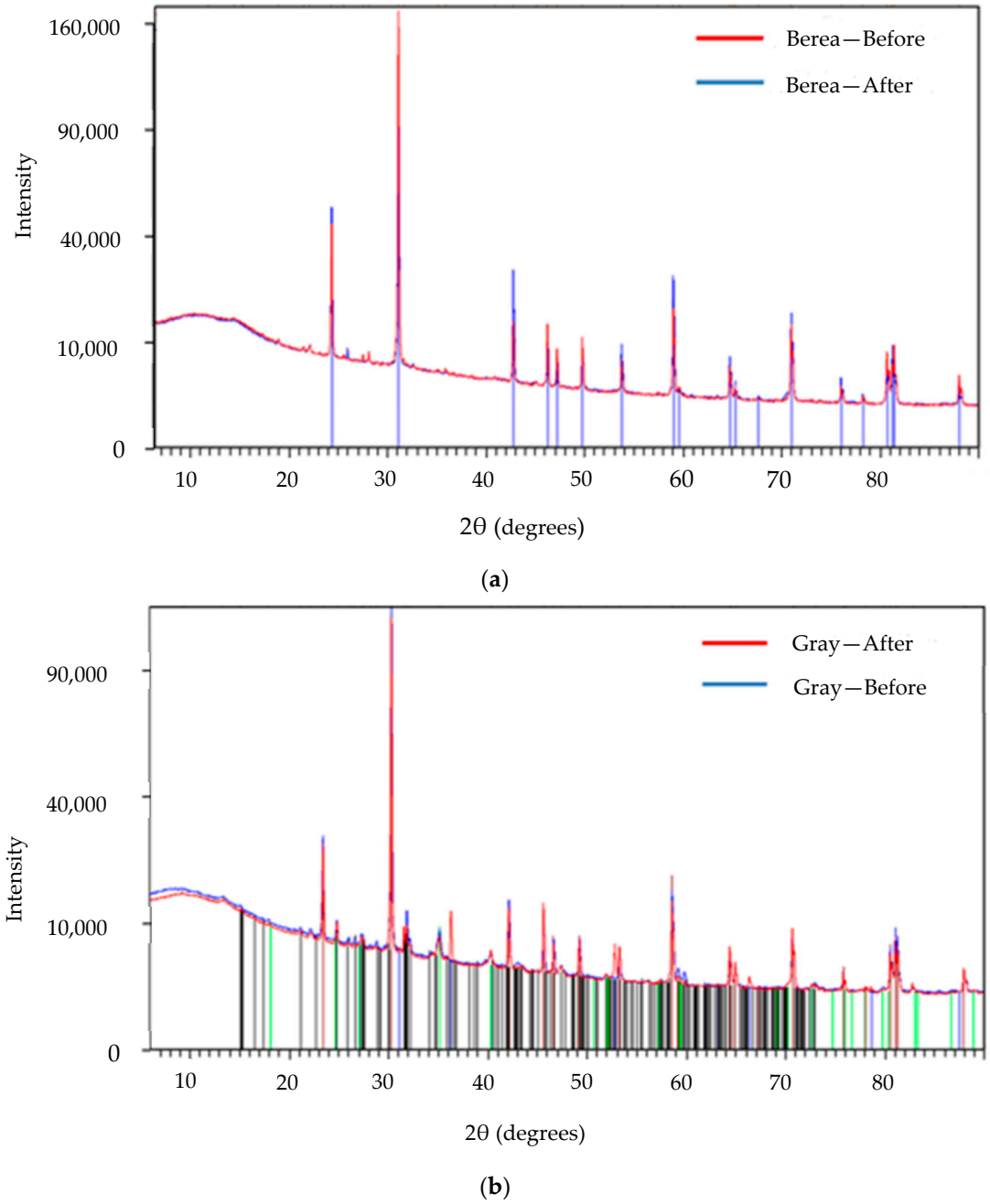


**Figure 7.** XRD Images for Berea's mineralogical composition (**a**) and Bandera Gray (**b**) before and after flooding.

### *3.2. Effect of Clay Content on Sandstone Trapping Capacity*

Rock wettability highly affects $CO_2$ vertical migration and $CO_2$ trapping capacities [6,9]. $CO_2$-wet rock has a significantly higher $CO_2$ upward mobility [69] and a much lower residual trapping capacity [9,24,70] for formations with adequate flow properties (such as permeability). Our results, presented in Section 3.1, show that $CO_2$ flooding in sandstones with a high clay content leads to the reservoir being $CO_2$-wet, which may lead to the above-listed detrimental mobility and storage effects. For example, based on the previous simulation study by [71], the $CO_2$ mobility is found to contribute by 0.5%, dissolution trapping capacity by 18.3%, and residual trapping capacity by 81.2% in the storage capacity of strongly water-wet rocks. By contrast, the strongly $CO_2$-wet rocks have a $CO_2$ mobility of 20.7%, dissolution trapping capacity of 28.6%, and residual trapping capacity of 50.7% after 10 years of storage (Figure 8).

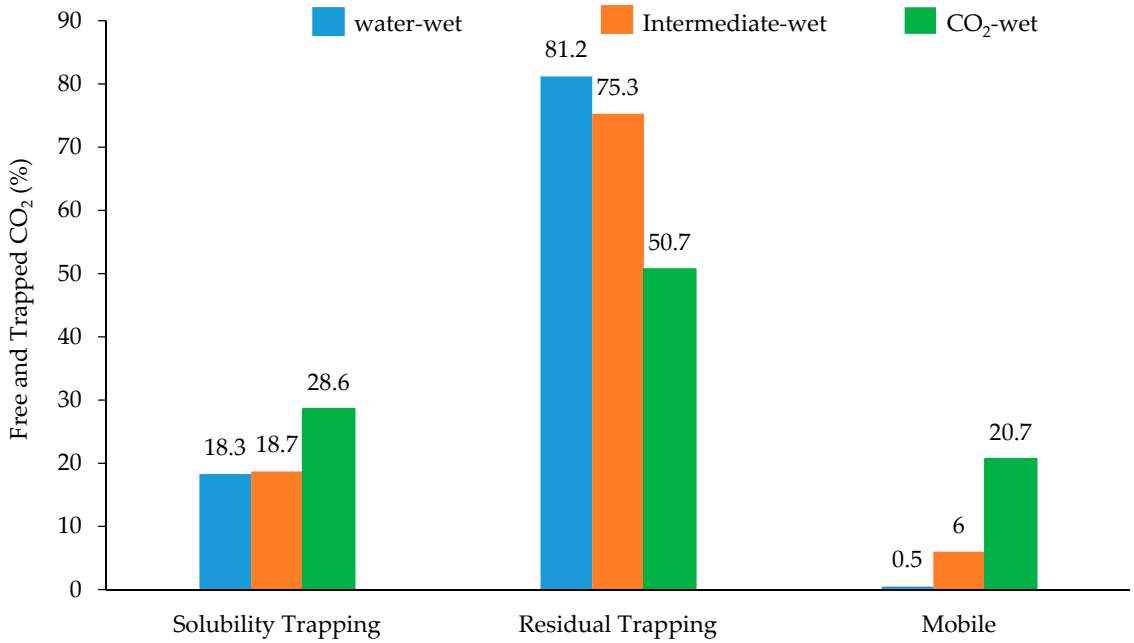


**Figure 8.** Percentages of free and trapped $CO_2$ capacities for strongly water-wet, intermediate-wet, and strongly $CO_2$-wet rocks (modified from [71]).

On the contrary, in formations with low permeability where the biggest challenge is the injection of $CO_2$, the enhanced $CO_2$ wetting of the rock's surface could be advantageous for pressure management provided there is a cap-rock that can make a good seal for containment security. The presence of high clay fractions in such low permeability formations will be beneficial for the enhanced $CO_2$ storage capacity by an increase in mobility, dissolution, and residual trapping.

## 4. Conclusions

Rock wettability has a significant role in carbon geo-sequestration (CGS). This is because the fluid flow through porous media is strongly controlled by rock wettability. Despite previous research on the area, the parameters influencing the $CO_2$/brine/rock wettability variation are still not fully understood. We thus systematically measured the contact angle (i.e., wettability) of two sandstones (i.e., low clay content (Berea) and high clay content (Bandera Gray)) before and after $CO_2$ flooding with brine (5 wt% NaCl + 1 wt% KCl in deionised water), $CO_2$-saturated (live) brine, and supercritical $CO_2$ ($scCO_2$), at 10 MPa and 15 MPa for a constant temperature (323 K). The results show that $CO_2$ flooding leads to an increase in the advancing and receding contact angles of both Berea and Bandera Gray sandstones (i.e., $CO_2$ flooding leads to increased $CO_2$-sandstone wettability). Our results also show that the $CO_2$/brine/rock contact angle increases with the pressure increase, which is in line with most of the literature data [18,20,59,60].

Moreover, our measurements demonstrate, for all tested conditions (both before and after the $CO_2$ flooding scenarios), that Berea sandstone has lower contact angles (i.e., more water wettability) than Bandera Gray (i.e., Bandera Gray tends to be more intermediate-wet to $CO_2$-wet), due to the higher clay content of Bandera Gray. Our SEM results show that the Bandera Gray sandstones, which became more $CO_2$-wet, contained a high clay content. The published literature indicates that, except for smectites, all clays are $CO_2$-adsorbing. Hence, sandstones with a high clay content become CO2-wet when flooded with $CO_2$, which results in the upward mobility of $CO_2$ in the reservoir, and consequently a reduced capillary trapping capacity. However, low permeability formations with significant $CO_2$ injection issues, $CO_2$-wetting of the reservoir rock surface, and an adequate seal for containment security could help improve the pressure management. Therefore, high clay fractions in such formations will be an advantage for the enhanced $CO_2$ storage capacity.

**Author Contributions:** Conceptualisation, C.A.F., A.A.-Y. and N.K.J.; methodology, C.A.F.; software, C.A.F. and E.A.-K.; validation, C.A.F., A.A.-Y. and N.K.J.; formal analysis, C.A.F.; investigation, C.A.F.; resources, C.A.F.; data curation, C.A.F.; writing—original draft preparation, C.A.F.; writing—review and editing, C.A.F. and H.R.A.; visualisation, C.A.F. and E.A.-K.; supervision, S.I., C.L. and A.B.; project administration, C.A.F.; funding acquisition, C.A.F. and A.B. All authors have read and agreed to the published version of the manuscript.

**Funding:** This research received no external funding.

**Institutional Review Board Statement:** Not applicable.

**Informed Consent Statement:** Not applicable.

**Data Availability Statement:** Not applicable.

**Acknowledgments:** Cut Aja Fauziah thanks the LPDP-Indonesia endowment fund for education, Ministry of Finance of the Republic of Indonesia, for sponsoring her study through the PhD scholarship.

**Conflicts of Interest:** The authors declare no conflict of interest.

## References

1. IPCC. Special Report on Carbon Dioxide Capture and Storage. In *Working Group III of the Intergovernmental Panel on Climate Change*; Metz, B., Davidson, O., Coninck, H.D., Loos, M., Meyer, L., Eds.; Cambridge University Press: Cambridge, UK; New York, NY, USA, 2005.
2. Pacala, S.; Socolow, R. Stabilization wedges: Solving the climate problem for the next 50 years with current technologies. *Science* **2004**, *305*, 968–972. [CrossRef]
3. Lackner, K.S.; Sachs, J. A robust strategy for sustainable energy. *Brook. Pap. Econ. Act.* **2005**, *2005*, 215–284. [CrossRef]
4. Deel, D.; Mahajan, K.; Mahoney, C.R.; McIlvried, H.G.; Srivastava, R.D. Risk assessment and management for long-term storage of $CO_2$ in geologic formations-United States Department of Energy R&D. *Syst. Cybern. Inf.* **2007**, *5*, 79–84.
5. Li, Q.; Liu, G. Risk assessment of the geological storage of $CO_2$: A review. In *Geologic Carbon Sequestration*; Vishal, V., Singh, T., Eds.; Springer: Cham, Switzerland, 2016; pp. 249–284.
6. Iglauer, S.; Al-Yaseri, A.Z.; Rezaee, R.; Lebedev, M. $CO_2$ wettability of caprocks: Implications for structural storage capacity and containment security. *Geophys. Res. Lett.* **2015**, *42*, 9279–9284. [CrossRef]
7. Hesse, M.A.; Woods, A. Buoyant dispersal of $CO_2$ during geological storage. *Geophys. Res. Lett.* **2010**, *37*, L01403. [CrossRef]
8. Pentland, C.H.; El-Maghraby, R.; Iglauer, S.; Blunt, M.J. Measurements of the capillary trapping of super-critical carbon dioxide in Berea sandstone. *Geophys. Res. Lett.* **2011**, *38*, L06401. [CrossRef]
9. Krevor, S.; Blunt, M.J.; Benson, S.M.; Pentland, C.H.; Reynolds, C.; Al-Menhali, A.; Niu, B. Capillary trapping for geologic carbon dioxide storage–From pore scale physics to field scale implications. *Int. J. Greenh. Gas. Con.* **2015**, *40*, 221–237. [CrossRef]
10. Ruprecht, C.; Pini, R.; Falta, R.; Benson, S.; Murdoch, L. Hysteretic trapping and relative permeability of $CO_2$ in sandstone at reservoir conditions. *Int. J. Greenh. Gas Control.* **2014**, *27*, 15–27. [CrossRef]
11. Suekane, T.; Nobuso, T.; Hirai, S.; Kiyota, M. Geological storage of carbon dioxide by residual gas and solubility trapping. *Int. J. Greenh. Gas Control.* **2008**, *2*, 58–64. [CrossRef]
12. Iglauer, S. Dissolution trapping of carbon dioxide in reservoir formation brine–A carbon storage mechanism. In *Mass Transfer Advanced Aspects*; Nakajima, H., Ed.; InTech Open: London, UK, 2011; pp. 233–262.
13. Emami-Meybodi, H.; Hassanzadeh, H.; Green, C.P.; Ennis-King, J. Convective dissolution of $CO_2$ in saline aquifers: Progress in modeling and experiments. *Int. J. Greenh. Gas Control.* **2015**, *40*, 238–266. [CrossRef]
14. Spycher, N.; Pruess, K.; Ennis-King, J. $CO_2$-$H_2O$ mixtures in the geological sequestration of $CO_2$. I. Assessment and calculation of mutual solubilities from 12 to 100 C and up to 600 bar. *Geochim. Cosmochim. Acta* **2003**, *67*, 3015–3031. [CrossRef]
15. Bachu, S.; Gunter, W.; Perkins, E. Aquifer disposal of $CO_2$: Hydrodynamic and mineral trapping. *Energ. Convers. Manage.* **1994**, *35*, 269–279. [CrossRef]
16. Gaus, I. Role and impact of $CO_2$–rock interactions during $CO_2$ storage in sedimentary rocks. *Int. J. Greenh. Gas Control.* **2010**, *4*, 73–89. [CrossRef]
17. Matter, J.M.; Stute, M.; Snæbjörnsdottir, S.Ó.; Oelkers, E.H.; Gislason, S.R.; Aradottir, E.S.; Sigfusson, B.; Gunnarsson, I.; Sigurdardottir, H.; Gunnlaugsson, E. Rapid carbon mineralization for permanent disposal of anthropogenic carbon dioxide emissions. *Science* **2016**, *352*, 1312–1314. [CrossRef] [PubMed]
18. Broseta, D.; Tonnet, N.; Shah, V. Are rocks still water-wet in the presence of dense $CO_2$ or $H_2S$? *Geofluids* **2012**, *12*, 280–294. [CrossRef]
19. Chiquet, P.; Broseta, D.; Thibeau, S. Wettability alteration of caprock minerals by carbon dioxide. *Geofluids* **2007**, *7*, 112–122. [CrossRef]
20. Iglauer, S.; Pentland, C.H.; Busch, A. $CO_2$ wettability of seal and reservoir rocks and the implications for carbon geo-sequestration. *Water Resour. Res.* **2015**, *51*, 729–774. [CrossRef]

21. Ali, M.; Arif, M.; Sahito, M.F.; Al-Anssari, S.; Keshavarz, A.; Barifcani, A.; Stalker, L.; Sarmadivaleh, M.; Iglauer, S. $CO_2$-wettability of sandstones exposed to traces of organic acids: Implications for $CO_2$ geo-storage. *Int. J. Greenh. Gas Control.* **2019**, *83*, 61–68. [CrossRef]
22. Abramov, A.; Iglauer, S.; Keshavarz, A. Wettability of fully hydroxylated and alkylated (001) alpha-quartz surface in carbon dioxide atmosphere. *J. Phys. Chem. C.* **2019**, *123*, 9027–9040. [CrossRef]
23. Chen, C.; Wan, J.; Li, W.; Song, Y. Water contact angles on quartz surfaces under supercritical $CO_2$ sequestration conditions: Experimental and molecular dynamics simulation studies. *Int. J. Greenh. Gas Control.* **2015**, *42*, 655–665. [CrossRef]
24. Niu, B.; Al-Menhali, A.; Krevor, S. A study of residual carbon dioxide trapping in sandstone. *Energy Procedia* **2014**, *63*, 5522–5529. [CrossRef]
25. Wiegand, G.; Franck, E.U. Interfacial tension between water and non-polar fluids up to 473 K and 2800 bar. *Ber. Bunsenges. Phys. Chem.* **1994**, *98*, 809–817. [CrossRef]
26. Yang, D.; Gu, Y.; Tontiwachwuthikul, P. Wettability determination of the crude oil−reservoir brine−reservoir rock system with dissolution of $CO_2$ at high pressures and elevated temperatures. *Energy Fuels* **2008**, *22*, 2362–2371. [CrossRef]
27. Arif, M.; Al-Yaseri, A.Z.; Barifcani, A.; Lebedev, M.; Iglauer, S. Impact of pressure and temperature on $CO_2$–brine–mica contact angles and $CO_2$–brine interfacial tension: Implications for carbon geo-sequestration. *J. Colloid Interface Sci.* **2016**, *462*, 208–215. [CrossRef]
28. Farokhpoor, R.; Bjørkvik, B.J.A.; Lindeberg, E.; Torsæter, O. Wettability behaviour of $CO_2$ at storage conditions. *Int. J. Greenh. Gas Control.* **2013**, *12*, 18–25. [CrossRef]
29. Espinoza, D.N.; Santamarina, J.C. Water-$CO_2$-mineral systems: Interfacial tension, contact angle, and diffusion—Implications to $CO_2$ geological storage. *Water Resour. Res.* **2010**, *46*, wo7537. [CrossRef]
30. Jha, N.K.; Iglauer, S.; Barifcani, A.; Sarmadivaleh, M.; Sangwai, J.S. Low-salinity surfactant nanofluid formulations for wettability alteration of sandstone: Role of the $SiO_2$ nanoparticle concentration and divalent cation/$SO_4^{2-}$ ratio. *Energy Fuels* **2019**, *33*, 739–746. [CrossRef]
31. Roshan, H.; Al-Yaseri, A.Z.; Sarmadivaleh, M.; Iglauer, S. On wettability of shale rocks. *J. Colloid Interface Sci.* **2016**, *475*, 104–111. [CrossRef]
32. Al-Yaseri, A.Z.; Sarmadivaleh, M.; Saidi, A.; Lebedev, M.; Barifcani, A.; Iglauer, S. $N_2$ + $CO_2$+ NaCl brine interfacial tensions and contact angles on quartz at $CO_2$ storage site conditions in the Gippsland basin, Victoria/Australia. *J. Pet. Sci. Eng.* **2015**, *129*, 58–62. [CrossRef]
33. Wiese, B.; Nimtz, M.; Klatt, M.; Kühn, M. Sensitivities of injection rates for single well $CO_2$ injection into saline aquifers. *Geochemistry* **2010**, *70*, 165–172. [CrossRef]
34. Ivanova, A.; Mitiurev, N.; Cheremisin, A.; Orekhov, A.; Kamyshinsky, R.; Vasiliev, A. Characterization of organic layer in oil carbonate reservoir rocks and its effect on microscale wetting properties. *Sci. Rep.* **2019**, *9*, 1–10. [CrossRef]
35. Carroll, S.A.; McNab, W.W.; Torres, S.C. Experimental study of cement-sandstone/shale-brine-$CO_2$ interactions. *Geochem. Trans.* **2011**, *12*, 9. [CrossRef]
36. Mohamed, I.M.; He, J.; Nasr-El-Din, H.A. Carbon dioxide sequestration in sandstone aquifers: How does it affect the permeability? In Proceedings of the Carbon Management Technology Conference, Orlando, FL, USA, 7–9 February 2012, CMTC-149958-MS.
37. Worden, R.H.; Smith, L.K. Geological sequestration of $CO_2$ in the subsurface: Lessons from $CO_2$ injection enhanced oil recovery projects in oilfields. *Geol. Soc. Lond. Spec. Publ.* **2004**, *233*, 211–224. [CrossRef]
38. Delle Piane, C.; Timms, N.E.; Saeedi, A.; Rezaee, M.R.; Mikhaltsevitch, V.; Lebedev, M.; Olierook, H. *Facies-Based Rock Properties Distribution Along the Harvey 1 Stratigraphic Well*; CSIRO Report Number EP133710; ANLEC: Barton, Australia, 2013.
39. Fischer, S.; Liebscher, A.; Wandrey, M.; Group, C.S. $CO_2$–brine–rock interaction—First results of long-term exposure experiments at in situ P–T conditions of the Ketzin $CO_2$ reservoir. *Chem. Erde-Geochem.* **2010**, *70*, 155–164. [CrossRef]
40. Lebedev, M.; Zhang, Y.; Sarmadivaleh, M.; Barifcani, A.; Al-Khdheeawi, E.; Iglauer, S. Carbon geosequestration in limestone: Pore-scale dissolution and geomechanical weakening. *Int. J. Greenh. Gas Control.* **2017**, *66*, 106–119. [CrossRef]
41. Jha, N.K.; Ivanova, A.; Lebedev, M.; Barifcani, A.; Cheremisin, A.; Iglauer, S.; Sangwai, J.S.; Sarmadivaleh, M. Interaction of low salinity surfactant nanofluids with carbonate surfaces and molecular level dynamics at fluid-fluid interface at $ScCO_2$ loading. *J. Colloid Interface Sci.* **2020**, *586*, 315–325. [CrossRef] [PubMed]
42. Li, P.; Zhang, J.; Rezaee, R.; Dang, W.; Li, X.; Fauziah, C.A.; Nie, H.; Tang, X. Effects of swelling-clay and surface roughness on the wettability of transitional shale. *J. Pet. Sci. Eng.* **2021**, *196*, 108007. [CrossRef]
43. Sigfusson, B.; Gislason, S.R.; Matter, J.M.; Stute, M.; Gunnlaugsson, E.; Gunnarsson, I.; Aradottir, E.S.; Sigurdardottir, H.; Mesfin, K.; Alfredsson, H.A. Solving the carbon-dioxide buoyancy challenge: The design and field testing of a dissolved $CO_2$ injection system. *Int. J. Greenh. Gas Control.* **2015**, *37*, 213–219. [CrossRef]
44. Ballentine, C.J.; Schoell, M.; Coleman, D.; Cain, B.A. 300-Myr-old magmatic $CO_2$ in natural gas reservoirs of the west Texas Permian basin. *Nature* **2001**, *409*, 327. [CrossRef] [PubMed]
45. Yu, H.; Zhang, Y.; Ma, Y.; Lebedev, M.; Ahmed, S.; Li, X.; Verrall, M.; Squelch, A.; Iglauer, S. $CO_2$ saturated brine injection into unconsolidated sandstone: Implications for carbon geo-sequestration. *J. Geophys. Res. Solid Earth.* **2019**, *124*, 10823–10838. [CrossRef]

46. Berrezueta, E.; González-Menéndez, L.; Breitner, D.; Luquot, L. Pore system changes during experimental $CO_2$ injection into detritic rocks: Studies of potential storage rocks from some sedimentary basins of Spain. *Int. J. Greenh. Gas Control.* **2013**, *17*, 411–422. [CrossRef]
47. Iglauer, S.; Sarmadivaleh, M.; Al-Yaseri, A.; Lebedev, M. Permeability evolution in sandstone due to injection of $CO_2$-saturated brine or supercritical $CO_2$ at reservoir conditions. *Energy Procedia* **2014**, *63*, 3051–3059. [CrossRef]
48. Lamy-Chappuis, B.; Angus, D.; Fisher, Q.; Grattoni, C.; Yardley, B.W. Rapid porosity and permeability changes of calcareous sandstone due to $CO_2$-enriched brine injection. *Geophys. Res. Lett.* **2014**, *41*, 399–406. [CrossRef]
49. Sayegh, S.; Krause, F.; Girard, M.; De Bree, C. Rock/fluid interactions of carbonated brines in a sandstone reservoir: Pembina Cardium, Alberta, Canada. *SPE Form. Eval.* **1990**, *5*, 399–405. [CrossRef]
50. Al-Yaseri, A.; Zhang, Y.; Ghasemiziarani, M.; Sarmadivaleh, M.; Lebedev, M.; Roshan, H.; Iglauer, S. Permeability evolution in sandstone due to $CO_2$ injection. *Energy Fuels* **2017**, *31*, 12390–12398. [CrossRef]
51. El-Maghraby, R.M.; Pentland, C.H.; Iglauer, S.; Blunt, M.J. A fast method to equilibrate carbon dioxide with brine at high pressure and elevated temperature including solubility measurements. *J. Supercrit. Fluids* **2012**, *62*, 55–59. [CrossRef]
52. Riaz, A.; Hesse, M.; Tchelepi, H.A.; Orr, F.M. Onset of convection in a gravitationally unstable diffusive boundary layer in porous media. *J. Fluid Mech.* **2006**, *548*, 87–111. [CrossRef]
53. Frykman, P.; Wessel-Berg, D. Dissolution trapping-convection enhancement limited by geology. *Energy Procedia* **2014**, *63*, 5467–5478. [CrossRef]
54. Emami-Meybodi, H.; Hassanzadeh, H.; Ennis-King, J. $CO_2$ dissolution in the presence of background flow of deep saline aquifers. *Water Resour. Res.* **2015**, *51*, 2595–2615. [CrossRef]
55. Love, J.C.; Estroff, L.A.; Kriebel, J.K.; Nuzzo, R.G.; Whitesides, G.M. Self-assembled monolayers of thiolates on metals as a form of nanotechnology. *Chem. Rev.* **2005**, *105*, 1103–1170. [CrossRef]
56. Iglauer, S.; Salamah, A.; Sarmadivaleh, M.; Liu, K.; Phan, C. Contamination of silica surfaces: Impact on water–$CO_2$–quartz and glass contact angle measurements. *Int. J. Greenh. Gas Control.* **2014**, *22*, 325–328. [CrossRef]
57. Lander, L.M.; Siewierski, L.M.; Brittain, W.J.; Vogler, E.A. A systematic comparison of contact angle. *Interface Sci.* **1991**, *141*, 275.
58. Fauziah, C.A.; Al-Yaseri, A.Z.; Beloborodov, R.; Siddiqui, M.A.; Lebedev, M.; Parsons, D.F.; Roshan, H.; Barifcani, A.; Iglauer, S. Carbon dioxide/brine, nitrogen/brine and oil/brine wettability of montmorillonite, illite and kaolinite at elevated pressure and temperature. *Energy Fuels* **2018**, *33*, 441–448. [CrossRef]
59. Fauziah, C.A.; Al-Yaseri, A.Z.; Jha, N.K.; Lagat, C.; Roshan, H.; Barifcani, A.; Iglauer, S. Carbon dioxide wettability of South West Hub sandstone, Western Australia: Implications for carbon geo-storage. *Int. J. Greenh. Gas Control.* **2020**, *98*, 103064. [CrossRef]
60. Arif, M.; Barifcani, A.; Iglauer, S. Solid/$CO_2$ and solid/water interfacial tensions as a function of pressure, temperature, salinity and mineral type: Implications for $CO_2$-wettability and $CO_2$ geo-storage. *Int. J. Greenh. Gas Control.* **2016**, *53*, 263–273. [CrossRef]
61. Siddiqui, M.A.Q.; Chen, X.; Iglauer, S.; Roshan, H. A multiscale study on shale wettability: Spontaneous imbibition versus contact angle. *Water Reso. Res.* **2019**, *55*, 5012–5032. [CrossRef]
62. Iqbal, M.A.; Salim, A.M.A.; Baioumy, H.; Gaafar, G.R.; Wahid, A. Identification and characterization of low resistivity low contrast zones in a clastic outcrop from Sarawak, Malaysia. *J. Appl. Geophy.* **2019**, *160*, 207–217. [CrossRef]
63. Schrader, M.E.; Yariv, S. Wettability of clay minerals. *J. Colloid Interface Sci.* **1990**, *136*, 85–94. [CrossRef]
64. Zhang, L.; Lu, X.; Liu, X.; Yang, K.; Zhou, H. Surface Wettability of Basal Surfaces of Clay Minerals: Insights from Molecular Dynamics Simulation. *Energy Fuels* **2016**, *30*, 149–160. [CrossRef]
65. Busch, A.; Bertier, P.; Gensterblum, Y.; Giesting, P.; Guggenheim, S.; Koster van Groos, A.; Weniger, P. Dioxide. In *3rd EAGE Shale Workshop-Shale Physics and Shale Chemistry*; European Association of Geoscientists & Engineers: Houten, The Netherlands, 2012.
66. Yu, M.; Liu, L.; Yang, S.; Yu, Z.; Li, S.; Yang, Y.; Shi, X. Experimental identification of $CO_2$–oil–brine–rock interactions: Implications for $CO_2$ sequestration after termination of a $CO_2$-EOR project. *Appl. Geochem.* **2016**, *75*, 137–151. [CrossRef]
67. Black, J.R.; Haese, R.R. Batch Reactor experimental results for GaMin'11: Reactivity of siderite/ankerite, labradorite, illite and chlorite under $CO_2$ saturated conditions. *Energy Procedia* **2014**, *63*, 5443–5449. [CrossRef]
68. Liu, R.; Heinemann, N.; Liu, J.; Zhu, W.; Wilkinson, M.; Xie, Y.; Wang, Z.; Wen, T.; Hao, F.; Haszeldine, R.S. $CO_2$ sequestration by mineral trapping in natural analogues in the Yinggehai Basin, South China Sea. *Mar. Pet. Geol.* **2019**, *104*, 190–199. [CrossRef]
69. Al-Khdheeawi, E.A.; Vialle, S.; Barifcani, A.; Sarmadivaleh, M.; Iglauer, S. Impact of reservoir wettability and heterogeneity on $CO_2$-plume migration and trapping capacity. *Int. J. Greenh. Gas Control.* **2017**, *58*, 142–158. [CrossRef]
70. Al-Menhali, A.S.; Menke, H.P.; Blunt, M.J.; Krevor, S.C. Pore scale observations of trapped $CO_2$ in mixed-wet carbonate rock: Applications to storage in oil fields. *Environ. Sci. Technol.* **2016**, *50*, 10282–10290. [CrossRef] [PubMed]
71. Al-Khdheeawi, E.A.; Vialle, S.; Barifcani, A.; Sarmadivaleh, M.; Iglauer, S. Influence of $CO_2$-wettability on $CO_2$ migration and trapping capacity in deep saline aquifers. *Greenh. Gases* **2017**, *7*, 328–338. [CrossRef]